Vibronic model for an ns^2 system: KCl:Au^-

D. Lemoyne, J. Duran, and M. Billardon
Laboratoire d'Optique Physique, 10 rue Vauquelin, 75231 Paris Cedex 05, France*

Le Si Dang
Laboratoire de Spectrométrie Physique,† Boîte Postale 53, 38041 Grenoble Cedex, France
(Received 8 December 1975)

The Au^- center in KCl is isoelectronic to the series of Tl^+-like ions. The electron-lattice coupling is sufficiently weak so that zero-phonon lines appear in the absorption spectra. Various perturbative optical measurements (stress and magnetically induced dichroism) were performed both in the zero-phonon line and in the vibronic continuum of the A band. Two independent sets of Jahn-Teller parameters have been obtained and found to be in complete agreement. Comparison of the results with existing theories clearly shows that this center exhibits a very interesting kind of Jahn-Teller effect where the system is equally coupled to the E_g and T_{2g} modes. It follows that the exact wave function of the lowest vibronic eigenstate has been obtained. In view of this model most of the features connected to the absorption band are derived.

I. INTRODUCTION

The existence of the Jahn-Teller effect in the ns^2-type ions, isoelectronic to the widely studied Tl^+ ion, was first suggested in a pioneer work by Seitz.[1] The problem was reconsidered more recently by Toyozawa and Inoue.[2] Dealing with the absorption-band shapes, these authors showed by an adiabatic and semiclassical approach to the problem, that the Jahn-Teller interaction could explain rather satisfactorily the three-peaked structure of several absorption bands in these systems. Their calculations were then extended by Cho[3] to various situations of Jahn-Teller coupling involving A_{1g}, E_g, and T_{2g} modes together. The computed absorption bands could in turn be compared to the experimental ones in order to get information about the detailed mechanism of the electron-lattice coupling.

After the publication of these papers, a great experimental effort was made in trying to determine the complete set of Jahn-Teller coupling parameters in various systems. Besides the study of the absorption-band shapes, perturbative measurements such as stress and magnetic dichroism were used.[4,5] Unfortunately, it turned out that in most cases the agreement between the various sets of parameters thus determined was recognized to be rather poor.

In parallel to this development of the studies concerning Tl^+-like ions, important progress was made towards the exact theoretical solution of the Jahn-Teller problem in cubic symmetry. Owing to the difficulty of solving for the complete vibronic Hamiltonian in the general situation of any coupling strength with A_{1g}, E_g, and T_{2g} modes, several limiting cases were investigated. First, the problem was solved in the case of a largely predominant coupling to E_g or T_{2g} mode only.[6] More recently the problem of the intermediate situation of equal coupling with E_g and T_{2g} modes could be solved by O'Brien[7] and Romestain and Merle D'Aubigné.[8] Their theory was applied successfully to the F^+ center in CaO (an electron trapped at a negative-ion vacancy), thus leading to a consistent model for this system.

Recently, an important work has been devoted to the fluorescence process of the ns^2 ions. It turned out that, due to the Jahn-Teller effect, the interpretation of the emission properties is rather complicated. In particular, it requires the knowledge of the exact vibronic wave function of the relaxed excited state. In fact, it was highly desirable to find a system in which the Jahn-Teller effect could be completely solved; unfortunately, none of the previously studied systems exhibited a sufficiently peculiar coupling so that any reliable comparison with the existing exact theories could be made.

The problem of finding an exact vibronic model for an ns^2 ion was reconsidered with the recent discovery of the Au^- system in alkali-halide crystals. These systems possess the interesting property of exhibiting a sufficiently weak electron-lattice coupling so as to show a zero-phonon line emerging from the vibronic continuum in the absorption spectrum. The existence of this zero-phonon line seemed to us quite promising for the research of a Jahn-Teller model, since it has been shown first by Ham[9] that perturbative experiments performed in this zero-phonon line lead to information about the lowest vibronic state. Thus, the aim of this paper was to investigate the Jahn-Teller effect of the KCl:Au^- system by using optical experiments performed both in the zero-phonon line and in the vibronic continuum, fol-

lowing a procedure which proved to be quite successful for the F^+ center in CaO.[10] In principle such experiments may be performed either in the C band or in the A band, since the electronic states of these two bands appear as known admixtures of $^1P_1$ and $^3P_1$ states. In this paper, we restricted ourselves to the A band (major contribution of $^3P_1$ state) for experimental convenience, since it lies closer to the visible than the C band.

Section II deals with the experimental setup, sample preparation, and technical procedures. Section III explains how the useful parameters have been extracted from the experimental data. In Sec. IV we show how our results may be analyzed in terms of a special case of Jahn-Teller effect. In Sec. V we put together some implications of the vibronic model and show how almost all the observed features of the absorption and dichroism curves can be explained. Finally, a brief discussion of the cluster model is reported in the Appendix.

II. EXPERIMENTAL

A. Sample preparation

KCl crystals containing various amounts of $AuHCl_4$ were grown by a Kyropoulos method at the Laboratoire de Physique Cristalline d'Orsay. The reduction into Au^- was made by solid-state electrolysis at a temperature of 610 °C and with currents of the order of 1 mA. This treatment introduces a large amount of F centers in the crystals. In order to bleach these centers, the crystals were kept at about 650 °C for a period of 12 h and then slowly cooled down to room temperature so as to minimize the effects of internal strains. Only the bulk of the crystals was kept for the experiments since, as was easily checked through absorption measurements, it contained only Au^- centers. The quantity of $AuHCl_4$ (roughly 1% by weight) added to the melt was chosen so that the maximum absorbance in the A band was ranging between 1 and 0.1 per mm.

B. Optical measurements

Magnetic circular dichroism (MCD) and stress linear dichroism experiments at various temperatures were performed on the broadband with the now classical technique using a photoelastic modulator and a gas-flow cryostat.[11] Measurements performed on the zero-phonon line required the use of a highly dispersive monochromator (bandwidth around 1 cm^{-1}). For an example, we report on Fig. 1 the spectra obtained for absorption and MCD experiments. It would have been necessary to deconvolute the measured absorption and MCD curves in order to obtain the correct values of the parameters. However, it may be shown that the use of the moments without any deconvolution introduces only a systematic error of about 6%. The actual bandwidth of the zero-phonon line turned out to be about 1.2 cm^{-1}, a value smaller than that obtained in Fischer's[12] work (~ 3.5 cm^{-1}). We infer from this result that our thermal treatment reduced the effects of the internal stresses.

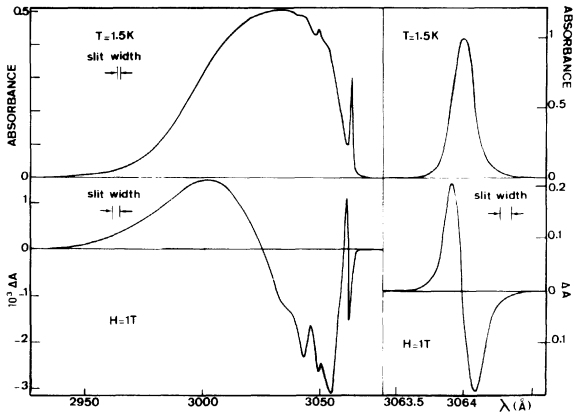

FIG. 1. Absorbance and corresponding dichroism signal in the broadband and in the zero-phonon line region.

III. ANALYSIS OF THE OPTICAL EXPERIMENTS

The excited electronic state corresponding to the so-called A band possesses T_{1u} symmetry ($J=1$) in the O_h point group. It is obtained by the mixing of the $^1P_1$ and $^3P_1$ states via spin-orbit mixing and is classically written

$$|Ai\rangle = -\nu|^1P_1 i\rangle + \mu|^3P_1 i\rangle .$$

When this electronic state is linearly coupled to the A_{1g}, E_g, and T_{2g} modes, the total vibronic Hamiltonian may be developed as

$$\mathcal{H}_V = (2\mu_A)^{-1}(P_\alpha^2 + \mu_A^2\omega_A^2 Q_\alpha^2) + V_A Q_\alpha \mathcal{J} + (2\mu_E)^{-1}[P_\theta^2 + P_\epsilon^2 + \mu_E^2\omega_E^2(Q_\theta^2 + Q_\epsilon^2)]$$

$$+ V_E(Q_\theta \mathcal{E}_\theta + Q_\epsilon \mathcal{E}_\epsilon) + (2\mu_T)^{-1}[P_\xi^2 + P_\eta^2 + P_\zeta^2 + \mu_T^2\omega_T^2(Q_\xi^2 + Q_\eta^2 + Q_\zeta^2)] + V_T(Q_\xi \mathcal{T}_{2\xi} + Q_\eta \mathcal{T}_{2\eta} + Q_\zeta \mathcal{T}_{2\zeta}) ,$$

where $\mathcal{J}, \mathcal{E}_g, \ldots, \mathcal{T}_{2\xi}$ are the usual matrices defined by Ham[9] and $V_\Gamma, \mu_\Gamma, \omega_\Gamma$ ($\Gamma = A, E, T$) are, respectively, the coupling coefficients, the effective masses, and the frequencies of the modes transforming like A_{1g}, E_g, and T_{2g}. The problem of finding a vibronic model will be undertaken by trying to measure pertinent parameters characteristic of the Jahn-Teller effect. Most of the experimental features may be connected to the Jahn-Teller energies corresponding to the minimum value of the potential energy in the vibronic $|Ai\rangle$ states:

$$E_{\mathrm{JT},E} = (\nu^2 - \tfrac{1}{2}\mu^2)^2 (V_E^2/2\mu_E\omega_E^2) = S_E\hbar\omega_E\,,$$
$$E_{\mathrm{JT},T} = (\nu^2 - \tfrac{1}{2}\mu^2)^2 (2V_T^2/3\mu_T\omega_T^2) = S_T\hbar\omega_T\,, \qquad (1)$$

and by analogy

$$E_{\mathrm{JT},A} = V_A^2/2\mu_A\omega_A^2 = S_A\hbar\omega_A\,.$$

These equations define unambigously the Huang-Rhys factors S_Γ.

From the experimental viewpoint, at least when the center is sufficiently weakly coupled, the Jahn-Teller effect appears both on the zero-phonon line and on the vibronic continuum. On the one hand, the zero-phonon line displays the properties of the well-defined lowest vibronic eigenstate and thus perturbative measurements performed in it will lead to an apparent reduction of the measured effects. This results from the so-called Ham[9] quenching factors. The measurements of these quenching factors associated to various external perturbations of T_{1g} symmetry (magnetic circular dichroism) and E_g and T_{2g} symmetries (stress linear dichroism for ⟨100⟩ and ⟨110⟩ stresses[10]) will give information about the vibrational part of the vibronic wave function of the lowest-excited state. On the other hand, the shape of the broadband also contains information about the electron-lattice coupling. The pertinent quantities which need to be calculated are then the successive moments of the absorption and dichroism spectra. As shown by Henry, Schnatterly, and Slichter,[13] (i) the first-order moment and first-order moment changes under external perturbations are related to purely electronic quantities; (ii) the second-order moment and third-order moment changes are connected to the electron-lattice coupling parameters S_Γ and to the effective phonon frequencies $\hbar\omega_\Gamma$.

In order to clarify the different processes which will lead to a vibronic model, we report in Table I a synoptic presentation of the extraction of the various useful parameters. The notations and definitions for the moments and moment changes follow those initially given in Ref. 13. For example, the first-order moment change induced

TABLE I. Synopsis of experiments and of extraction of parameters processes.

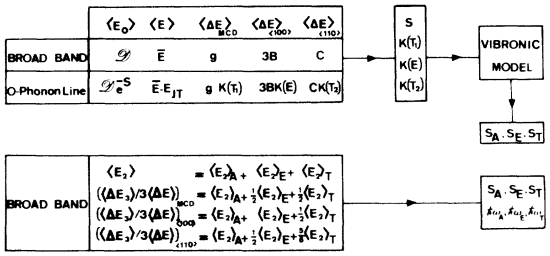

by stresses applied along ⟨100⟩ and ⟨110⟩ will be respectively measured by

$$\langle\Delta E\rangle_{\langle 100\rangle} = \langle E\rangle_{\langle 100\rangle} - \langle E\rangle_{\langle 010\rangle}\,,$$
$$\langle\Delta E\rangle_{\langle 110\rangle} = \langle E\rangle_{\langle 110\rangle} - \langle E\rangle_{\langle 1\bar{1}0\rangle}\,,$$

the subscripts referring to light polarization parallel and perpendicular to the applied stress.

A. Combined zero-phonon line and broadband experiments

The measurements of the zeroth- and first-order moments ($\langle E\rangle_0$ and $\langle E\rangle$) of the absorption band lead to the dipole strength $\mathcal{D}$ and the electronic transition energy $\bar{E}$. The first-order moment changes under a magnetic field and stresses will lead, respectively, to the Landé factor g of the A states and to the splitting coefficients $3B$ and C defined by Kaplianskii.[14] These coefficients are given by

$$\langle\Delta E\rangle_{\mathrm{MCD}} = 2g\mu_B H\,, \quad \langle\Delta E\rangle_{\langle 100\rangle} = 3Bp\,, \quad \langle\Delta E\rangle_{\langle 110\rangle} = Cp\,,$$

where H and p represent the magnetic field and the applied stress.

According to Table I the same moment and moment change measurements performed in the zero-phonon line will lead to the determination of S ("total" Huang-Rhys factor), E_{JT} ("total" Jahn-Teller energy defined as the energy distance between the zero-phonon line and the centroid of the band), and $K(T_1)$, $K(E)$, and $K(T_2)$ which are the quenching factors associated, respectively, with the magnetic, stress along ⟨100⟩, and stress along ⟨110⟩ perturbations. Experimentally, we found[15]

$E_{\mathrm{JT}} = 440 \pm 20$ cm^{-1}; $S = 4.8 \pm 0.5$;

$g = 1.45 \pm 0.15$; $K(T_1) = 0.24 \pm 0.04$;

$3B = -2.93 \pm 0.3$ cm^{-1}/(kg/mm^2); $K(E) = 0.58 \pm 0.08$;

$C = -5.72 \pm 0.6$ cm^{-1}/(kg/mm^2); $K(T_2) = 0.53 \pm 0.08$.

B. Broadband experiments

The Huang-Rhys factors S_Γ and the effective phonon frequencies $\hbar\omega_\Gamma$ may be extracted from the group of relations reported in Table I, where the $\langle E_2\rangle_\Gamma$ are given by

$$\langle E_2\rangle_A = S_A(\hbar\omega_A)^2 \coth(\hbar\omega_A/2kT)\,,$$
$$\langle E_2\rangle_E = S_E(\hbar\omega_E)^2 \coth(\hbar\omega_E/2kT)\,, \qquad (3)$$
$$\langle E_2\rangle_T = \tfrac{3}{2} S_T(\hbar\omega_T)^2 \coth(\hbar\omega_T/2kT)\,.$$

They represent the contributions of the various lattice modes to the bandwidth. Figure 2 reports the temperature dependence of the pertinent moments. Our experimental curves combined with the equations of Table I lead to

$$S_A = 3.8 \pm 0.4;\quad S_E = S_T = S_{NC} = 0.72 \pm 0.08\,;$$
$$\hbar\omega_A = 65 \pm 7 \text{ cm}^{-1};\quad \hbar\omega_E = \hbar\omega_T = \hbar\omega_{NC} = 160 \pm 16 \text{ cm}^{-1}\,;$$
$$E_{JT,A} = 247 \pm 50 \text{ cm}^{-1};$$
$$E_{JT,E} = E_{JT,T} = E_{JT,NC} = 115 \pm 25 \text{ cm}^{-1}\,.$$

A particularly interesting result consists of the equality of the Jahn-Teller energies corresponding to the noncubic (NC) E_g and T_{2g} modes. This may also be found directly when considering the curves reported in Fig. 2. Actually, it is observed that the curves corresponding to $(\langle \Delta E_3\rangle/3\langle \Delta E\rangle)_{\langle 100\rangle}$ and $(\langle \Delta E_3\rangle/3\langle \Delta E\rangle)_{\langle 110\rangle}$ are superimposed within the experimental error limits. Considering the equations of Table I, this may occur only if $\langle E_2\rangle_T \equiv \frac{3}{2}\langle E_2\rangle_E$. The use of Eqs. (3) then shows that $E_{JT,E} = E_{JT,T}$.

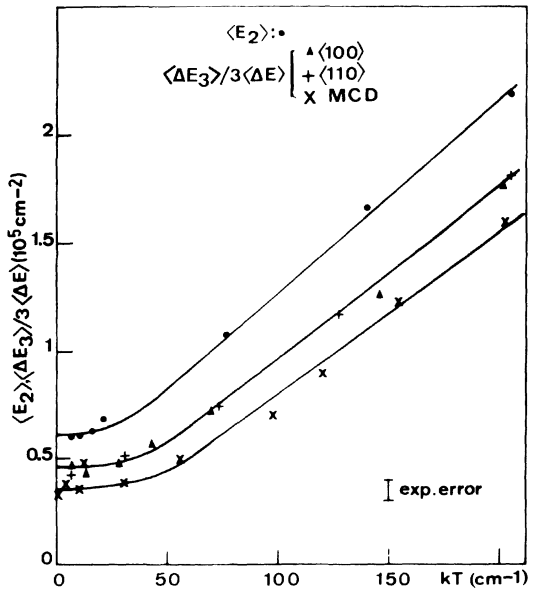

FIG. 2. Temperature dependence of the moments of the broadbands involved in the determination of the S_Γ and $\hbar\omega_\Gamma$ parameters (see text).

IV. VIBRONIC MODEL

The emerging feature of the preceding results is the equality of the coupling with the noncubic modes. This peculiar case of a triplet electronic state equally coupled to tetragonal and trigonal modes has already been observed in the F^+ center in CaO. The corresponding theoretical problem has received much attention these last years and exact solutions have been derived for the diagonalization of the vibronic Hamiltonian, at least for the lowest vibronic eigenstate (O'Brien,[7] Romestain and Merle D'Aubigné[8]). The KCl:Au^- system appearing as a good test for these theories, we have compared our results to the theoretical predictions. For this purpose, we have assumed that the $|Ai\rangle$ states have pure T_{1u} symmetry, neglecting the mixing with the $|{}^3P_2 j\rangle$ states through Jahn-Teller coupling (see Sec. V A), since the existing theories have been elaborated in this case. The theory of the D-mode model (E_g and T_{2g} modes degenerate in a five-dimensional oscillator) predicts that two general relationships exist between the reduction factors $K(T_1)$, $K(E)$, and $K(T_2)$. These are

$$K(E) = K(T_2),\quad 5K(E) = 3K(T_1) + 2\,,$$

whatever the coupling strengths are. Actually, we find that the difference between the measured values of $K(E)$ and $K(T_2)$ is smaller than the experimental errors. If we now calculate $K(T_1)$ using 0.55 as a mean value for $K(E) = K(T_2)$ we find

$$K(T_1) = 0.25\,,$$

which agrees with our experimental result. This agreement between the theoretical predictions of the D-mode model and our results give a strong support to this model for KCl:Au^-.

We can go further with this model and calculate the corresponding S_Γ Huang-Rhys factors starting

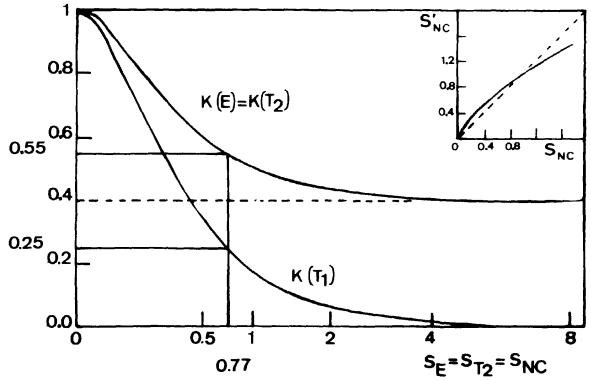

FIG. 3. Reduction factors plotted against the strength of the Jahn-Teller coupling. Insert is a plot of S'_{NC} vs S_{NC} [after O'Brien (Ref. 7)].

TABLE II. Comparison of the Huang-Rhys factors obtained from the broadband and zero-phonon line experiments.

S factors	Broadband	0-phonon line + D-mode model
S_A	3.8	4.0
S_E	0.72	0.77
S_T	0.72	0.77

from our measured values for $K(T_1)$, $K(E)$, and $K(T_2)$. This calculation may be performed by using formulas given in Ref. 8. However, for sake of illustration, we preferred using a curve computed by O'Brien[7] which we have reproduced in Fig. 3. This curve connects the $S_E = S_T$ parameters with the quenching factors. Our results give

$$S_E = S_T = S_{NC} = 0.77 \pm 0.09 .$$

From this value of the Huang-Rhys parameters, we may derive the effective S factor S'_{NC}, which is active in the reduction of the zero-phonon line intensity (insert of Fig. 3). This allows the evaluation of the S_A factor connected to the S of Table I by

$$S_A = S - S'_{NC} = 4.0 \pm 0.6 .$$

We now possess the complete set of S_Γ parameters derived from our experiments using the D-mode model. It is worth comparing these parameters to those obtained previously using broadband experiments. The results are gathered in Table II. The remarkable agreement between the sets of S_A, S_E, and S_T values obtained by two independent methods shows the high consistency of this vibronic model for the KCl:Au$^-$ system. We wish now to examine some interesting features which can also be discussed in the light of this model.

V. DISCUSSION

A. Relative order of magnitude of spin-orbit and Jahn-Teller energies

One might raise the question to know whether the spin-orbit energy is sufficiently large compared to the Jahn-Teller effect so as to ensure that we may effectively use the D-mode model established for a pure T_{1u} state. In fact, it appears that the bandwidth of the A band is of the same order of magnitude as the spin-orbit energy (about 1600 cm^{-1}). Thus, at the beginning of this study, this feature appeared to us a great source of difficulties. Fortunately, the problem was overcome when our results proved that the important enlargement of the band was due mostly to the cubic mode A_{1g}. The order of the successive diagonalization for the spin-orbit and vibronic Hamiltonians is governed by the relative importance of the spin-orbit energy and the Jahn-Teller energy corresponding to the *noncubic* modes. Our results indicate that this Jahn-Teller energy is smaller than the spin-orbit coupling constant by a factor of 14. This explains why the D-mode model can be applied to our system.

B. Mixing of the $|Ai\rangle$ states with the $|^3P_2 j\rangle$ states

Since the transition between the ground state and the $^3P_2$ state is allowed through the electron-lattice interaction, the mixing appears as a temperature-dependent part in the dipole strength $\mathfrak{D}$ of the A band. In view of the preceding model, we can now calculate thoroughly this contribution and compare it to the experimental result. Treating the mixing between the $|Ai\rangle$ and $|^3P_2 j\rangle$ states as a perturbation, we find

$$\mathfrak{D}(T) = \mathfrak{D}\left(1 - \mu^2 \left| \sum_j \frac{\langle {}^3P_2 j | \mathcal{H}_V | {}^3P_1 i \rangle}{E_{BA}} \right|^2 \right)$$

$$= \mathfrak{D}\left(1 - 1.75 \frac{S_{NC} (\hbar\omega_{NC})^2}{E_{BA}^2} \coth \frac{\hbar\omega_{NC}}{2kT}\right) .$$

Since we know all the parameters involved in this formula we can calculate the ratio $\mathfrak{D}(T)/\mathfrak{D}(0)$. A good agreement is obtained with the experimental values as reported in Fig. 4.

C. Position of the lowest vibronic eigenstates

The quantity which we called "total" Jahn-Teller energy E_{JT} is measured by the distance between the zero-phonon line and the centroid of the A band. Since we know now the characteristic parameters that are related to the Jahn-Teller effect, we should be able to recalculate E_{JT}. The noncubic modes act in displacing the lowest vibronic level through an effective $(S_{NC})_{eff}$ Huang-Rhys factor that is related to S_{NC} via the vibronic model. We can write

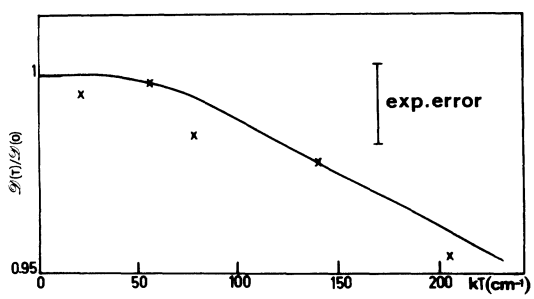

FIG. 4. Temperature dependence of the dipole strength of the A band: experimental data (×) and theoretical curve (see text).

$$E_{JT} = S_A \hbar\omega_A + (S_{NC})_{eff} \hbar\omega_{NC} .$$

Using the calculations of O'Brien,[7] we find $(S_{NC})_{eff} = 1.26$ leading to $E_{JT} = 455$ cm^{-1} which compares favorably to the experimental value of 440 cm^{-1}.

D. Landé factor g of the electronic $|Ai\rangle$ states

It is worth noting the large value of 1.45 which we obtained in our experiments for g. This result is to be compared to the results of similar experiments performed on other systems of the Tl^+ series where g was found to range between 0.1 and 0.8. Using a formula established by Honma,[16] we can calculate the orbital Landé factor[17] g_{orb}:

$$g_{orb} = (g - \mu^2)/(\nu^2 + \tfrac{1}{2}\mu^2) .$$

Using $\mu^2/\nu^2 = 14$ (Ref. 12), we find $g_{orb} = 0.97$ which is remarkably close to that of the free ion ($g_{orb} = 1$). This result proves that no significant reduction effect exists in this system. This feature may indicate that the electronic system is rather localized in its excited state inside a cluster of its nearest neighbors. It is therefore interesting to check the validity of the cluster model. We have reported its discussion in the Appendix.

E. Absorption band shape

As has been first noted by Hughes,[18] the case of equal coupling of a triplet state to both E_g and T_{2g} modes leads to a very particular absorption-band shape which turns out to be rather "flat topped" as in the case of CaO:F^+. This argument seems to disagree with our results since the band shape of KCl:Au^- looks much more triangular than that of CaO:F^+. As indicated by Hughes[18] the relevant parameter which needs to be calculated in order to get an idea of the squareness of the absorption curve is the ratio $\langle E_4\rangle/\langle E_2\rangle^2$. Performing the calculation, one obtains for the two limit cases of a rectangular and Gaussian distribution, respectively, 1.8 and 3. The case of CaO:F^+ (2.1) interpolates between these two cases much closer to the rectangular band shape, whereas KCl:Au^- (2.8) appears to be much more Gaussian-like. This feature may be understood quite easily by considering the large preponderance of the electron-lattice coupling with the A_{1g} modes in the case of KCl:Au^-. Then one expects an absorption curve looking much like those calculated by O'Brien[7] in the case of $p \rightarrow s$ transitions, which is effectively what is observed.

VI. CONCLUSION

The emerging result of this study consists of a well-defined vibronic model for the KCl:Au^- system. On the one hand, the D-mode model implies both the equality of the Huang-Rhys parameters for the E_g and T_{2g} modes and the equality of the phonon frequencies. This double equality could be looked upon as fortuitous if it had not been already observed in the case of the CaO:F^+ center and also perhaps for the F center in some alkali-halides (Hughes[18]). Such a striking result has not received any physical explanation so far. On the other hand, this D-mode model, confirmed through a certain number of experimental features, provides a reliable basis for future fluorescence experiments. Actually, the exact wave functions of the lowest vibronic state may be calculated exactly using the formulas given in Ref. 8. This, in turn may be used for the calculation of the selection rules governing the polarization properties of the fluorescence light. In particular, the "orbit memory," corresponding to the linear fluorescence polarization ratio under polarized excitation may be predicted using this wave function. However, it should be noted that at very low temperature (e.g., 1 K), polarization properties of the emitted light are greatly dependent on the random internal stresses. Owing to the Boltzman factor, if the relaxation time is small compared to the lifetime of the $|Ai\rangle$ relaxed excited state [measured as 0.3 μ sec (Ref. 19)], energy splittings as small as 1 cm^{-1} should be efficient in depopulating some of the Jahn-Teller wells and thus change the selection rules governing the polarization of the emitted light. From this point of view an interesting feature of the KCl:Au^- system turns out to be the relatively small bandwidth of the zero-phonon line compared to that of other weakly-coupled color centers. Supposing that the enlargement of the zero-phonon line is mainly due to the internal strains, we can roughly estimate the mean value of tetragonal and trigonal stresses to be smaller than 0.7 and 0.4 kg/mm^2.

ACKNOWLEDGMENTS

Thanks are owing to Professor J. P. Chapelle who kindly supplied the crystals used in this study and to Dr. Y. Merle d'Aubigné and Dr. R. Romestain for fruitful discussions on the subject.

APPENDIX: CLUSTER MODEL

The following relationships,

$$V_1 = 3(C_{11} + 2C_{12})A; \quad V_2 = \tfrac{2}{3}(C_{11} - C_{12})3B; \quad V_3 = 2C_{44}C \tag{A1}$$

connect the unquenched Kaplianskii's[14] stress coefficients A, $3B$, and C to the corresponding

strain coefficients V_i. We try to compare the V_i's to the dynamic parameters V_Γ. This is possible if one assumes that the interaction with the lattice is limited to one shell of neighbors, that is, if the cluster model is valid. Indeed, when the six K^+ nearest neighbors are at a distance R from the center of the vacancy, the coefficients defined by

$$V_1' = \sqrt{6}\, V_A R\,,$$
$$V_2' = 2(\nu^2 - \tfrac{1}{2}\mu^2) V_E R/\sqrt{3}\,, \qquad \text{(A2)}$$
$$V_3' = 2(\nu^2 - \tfrac{1}{2}\mu^2) V_T R$$

should be equal to the corresponding V_1, V_2, and V_3 coefficients. The comparison of these two sets of coefficients is made in Table III.

In spite of the crudeness of the model the V_1' and V_2' thus calculated compare rather well with the static parameters. The agreement between V_3 and V_3' is not as good. Following the arguments developed by Schnatterly,[20] it can be seen that the agreement would be better if one took account of the interaction with both first and second shells moving out of phase in an optical mode. Another explanation for the difference of V_3 and V_3' is that the "local" stiffness constant C_{44} would be larger than that of the host matrix.

TABLE III. Strain coefficients: (a) measured, the local stiffness constants [Eq. (A1)] being assumed to be equal to the bulk ones; (b) calculated using Eqs. (1), (2), and (A2). The effective mass was taken to be equal to the mass of the cation.

Strain symmetry	Strain coefficients/10^3 cm^{-1} (a)	(b)
A_{1g}	$V_1 = 13.9$	$\lvert V_1' \rvert = 12.2$
E_g	$V_2 = -8.4$	$\lvert V_2' \rvert = 9.7$
T_{2g}	$V_3 = -7.6$	$\lvert V_3' \rvert = 14.6$

*Research Group No. 5 of the CNRS.
†Laboratory No. 8 associated with the CNRS.
[1]F. Seitz, J. Chem. Phys. 6, 150 (1938).
[2]Y. Toyozawa and M. Inoue, J. Phys. Soc. Jpn. 21, 1663 (1966).
[3]K. Cho, J. Phys. Soc. Jpn. 25, 1372 (1968).
[4]K. Cho, J. Phys. Soc. Jpn. 27, B46 (1969).
[5]J. Duran, J. Badoz, and S. Pauthier-Camier, J. Phys. (Paris) 32, 973 (1971).
[6]Review articles of the Jahn-Teller effect in solids can be found in: F. S. Ham, in *Electron Paramagnetic Resonance*, edited by S. Geshwind (Plenum, New York, 1970); M. D. Sturge, in *Solid State Physics*, edited by F. Seitz and D. Turnbull (Academic, New York, 1967), Vol. 20.
[7]M. C. M. O'Brien, J. Phys. C 4, 2524 (1971).
[8]R. Romestain and Y. Merle d'Aubigné, Phys. Rev. B 4, 4611 (1971).
[9]F. S. Ham, Phys. Rev. 138, A1727 (1965).
[10]J. Duran, Y. Merle d'Aubigné, and R. Romestain, J. Phys. C 5, 2225 (1972).
[11]J. Badoz, M. Billardon, B. Briat, and A. C. Boccara, Trans. Faraday Soc. 3, 27 (1970).
[12]F. Fischer, Z. Phys. (Leipz.) 231, 293 (1970).
[13]C. H. Henry, S. E. Schnatterly, and C. P. Slichter, Phys. Rev. 137, A 583 (1965).
[14]A. A. Kaplianskii, Opt. Spektrosk. 16, 1031 (1964) [Opt. Spectrosc. 16, 557 (1964)].
[15]We used Fischer's (see Ref. 12) data for the stress experiments in the zero-phonon line.
[16]A. Honma, J. Phys. Soc. Jpn. 24, 1082 (1968).
[17]Honma (see Ref. 16) takes into account the magnetic mixing between the $|Ai\rangle$ and $|{}^3P_2 j\rangle$. In our case the resulting temperature-dependent deviation is found to be smaller than 5% and therefore neglected.
[18]A. E. Hughes, J. Phys. C 3, 627 (1970).
[19]K. Shigematsu and R. Onaka, Sci. Light 23, 27 (1974).
[20]S. E. Schnatterly, Phys. Rev. 140, A1364 (1965).